Article

Not peer-reviewed version

Optimization of a Modular Nanotransporter Design for the Killing of Cancer Cells via Targeted Intracellular Delivery of a Photosensitizer

Rena T. Alieva , Alexey V. Ulasov , Yuri V. Khramtsov , Taniana A. Slastnikova , Tatiana N. Lupanova , Maria A. Gribova , Georgii P. Georgiev , Andrey A. Rosenkranz *

Posted Date: 16 July 2024

doi: 10.20944/preprints202407.1330.v1

Keywords: modular nanotransporters; targeted drug delivery; photosensitizers; anticancer drugs; photodynamic effect; epidermal growth factor receptors; binding; importins; Keap1

Article

Optimization of a Modular Nanotransporter Design for the Killing of Cancer Cells Via Targeted Intracellular Delivery of a Photosensitizer

Rena T. Alieva [1], Alexey V. Ulasov [1], Yury V. Khramtsov [1], Tatiana A. Slastnikova [1], Tatiana N. Lupanova [1], Maria A. Gribova [2], Georgii P. Georgiev [1] and Andrey A. Rosenkranz [1,2,*]

[1] Laboratory of Molecular Genetics of Intracellular Transport, Institute of Gene Biology of Russian Academy of Sciences, 34/5 Vavilov St., 119334 Moscow, Russia
[2] Faculty of Biology, Lomonosov Moscow State University, 1-12 Leninskie Gory St., 119234 Moscow, Russia
* Correspondence: aar@genebiology.ru

Abstract: Modular nanotransporters (MNTs) are drug delivery systems for targeted cancer treatment. Being composed of several modules, they offer the advantage of high specificity and biocompatibility in delivering drugs to the target compartment of cancer cells. The large carrier module brings together functioning MNT modules and serves as a platform for drug attachment. The development of smaller-sized MNTs via truncation of the carrier module looks advantageous in facilitating tissue penetration. In this study, two new MNTs with a truncated carrier module containing either an N-terminal (MNT_N) or a C-terminal (MNT_C) part were developed by genetic engineering. Both new MNTs demonstrated high affinity for target receptors, as revealed by fluorescently labeled ligand-competitive binding. The liposome leakage assay proved the endosomolytic activity of MNTs. Binding to the importin heterodimer of each truncated MNT was revealed by a thermophoresis assay, while only MNT_N possessed binding to Keap1. Finally, the photodynamic efficacy of the photosensitizer attached to MNT_N was significantly higher than when attached to either MNT_C or the original MNT. Thus, this work reveals that MNT's carrier module can be truncated without losing MNT functionality, favoring the N-terminal part of the carrier module due to its ability to bind Keap1.

Keywords: modular nanotransporters; targeted drug delivery; photosensitizers; anticancer drugs; photodynamic effect; epidermal growth factor receptors; binding; importins; Keap1

1. Introduction

One of the most essential factors in effective cancer treatment is its ability to act specifically on tumor cells [1]. Therefore, the development of targeted drug delivery systems represents a promising area to obtain more effective anticancer treatment modalities [2]. Polypeptide constructs as drug carriers for targeting intracellular sites are advantageous due to their high specificity and biocompatibility. However, they often face challenges such as rapid degradation and low bioavailability, mainly because of the necessity to penetrate lipid membranes [3–6]. One of these systems is modular nanotransporters (MNTs), which are artificial polypeptides composed of several transport modules [7]. MNTs are capable of increasing the efficiency of the delivery of cytotoxic agents into the nuclei of cancer target cells, which greatly enhances the effectiveness of photodynamic therapy (PDT) [8, 9] and radionuclide therapy [10, 11]. PDT is an emerging treatment method for skin neoplasms and a number of solid tumors, including esophagus, lung, and prostate cancers [12–14]. PDT employs substances that can mediated a transition to an excited state in response to light, producing reactive oxygen species (ROS) that cause biomolecule damage, activation of the immune response, and cell death [13, 15, 16]. ROS with a short lifetime lead to damage in the nanometer range from the place of their generation; therefore, intracellular delivery to the most damage-sensitive structures of cancer cells is necessary for maximum efficiency. Previous studies

 doi:10.20944/preprints202407.1330.v1

have demonstrated that delivering photosensitizers to cancer cell nuclei via MNT can increase their photodynamic activity by up to 2,500 times [17].

Each module of MNT provides a particular stage of transport when MNT enters the target cell and then relocates to a specified cell compartment. MNTs, unlike many other therapeutic polypeptides, can permeate membranes and reach the cytosol of target cells. The sequences of MNT modules derived from natural proteins are united in a single gene sequence that encodes a chimeric protein capable of delivering drugs to a specified location of the target cell. MNT modules are interchangeable, allowing for customization based on the target cell type and the desired intracellular location for drug delivery [7]. Depending on their composition, MNT can penetrate, for example, cell nuclei, lysosomes, or bind to the surface of mitochondria [7, 11, 17, 18]. They contain a ligand module that binds to overexpressed cell surface receptors, allowing it to recognize a specified cell type. Receptor-mediated endocytosis leads to the internalization of MNT, and for subsequent release from endosomes, MNT contains an endosomolytic module capable of destroying lipid membranes in a slightly acidic environment within endosomes. MNT can also contain modules for transport to a specific cellular compartment, most commonly a nuclear localization signal (NLS) for the delivery of drugs into the nucleus [7]. The carrier module combines functionally active MNT modules and is also used to attach drugs that are transported by the transporter. Most of the MNT constructs developed to date use the hemoglobin-like protein (HMP, [19]) from *Escherichia coli* as the carrier module. Reducing the size of macromolecules facilitates diffusion in tissues, which contributes to a greater depth of penetration and, consequently, better delivery of the active principle [20]. HMP performs the function of a carrier and does not play a significant role in interaction with cellular structures during transport into the target cell compartments. Therefore, in order to reduce the size of MNT, it may be reasonable to consider truncating this module. HMP has two domains: the beta-folded C-terminal domain and the alpha-helical N-terminal globin domain with a pocket for porphyrin [20]. Keeping one of these HMP domains as a carrier module allows us to create a smaller construct. Because a crucial function of the carrier module is to ensure the availability of the MNT's endosomolytic and ligand modules for interaction with cellular structures, it requires truncation without compromising their activity.

Another rationale for the development of constructs with a truncated carrier module is the recently discovered interaction of HMP, which is part of one of the MNTs, with Kelch-like ECH-associated protein 1 (Keap1) [18]. Keap1 is widely represented in the cytoplasm and is involved in the control of many cellular activities, primarily the regulation of the level of transcription factor NF-E2-related factor 2 (Nrf2) [21–23]. In addition, Keap1 interacts with the PGAM5 protein, which is localized on the outer membrane of mitochondria and is also involved in maintaining mitochondrial homeostasis [24, 25]. Interaction with Keap1 can lead to the retention of MNT in the cytoplasm and the activation of cell signaling pathways, resulting in defense from the oxidative process. On the other hand, through the interaction of MNT with Keap1, it is possible to target cytotoxic agents to mitochondria. As demonstrated in our recent work, attaching a photosensitizer to MNT with the anti-Keap1 monobody sequence increases photocytotoxicity compared to a photosensitizer attached to a cytosol-targeted MNT [18]. Thus, the development and study of new MNT will shed light on the possibilities of creating functional MNT structures in smaller sizes. Furthermore, this allows us to examine the effect of an additional mitochondrial localization site on the photocytotoxicity of photosensitizers delivered to the nucleus of a cancer target cell.

2. Materials and Methods

2.1. Cell Lines

The human epidermoid carcinoma A431 cell line was obtained from the American Type Culture Collection (ATCC, Manassas, VA, USA) and maintained according to the ATCC specification.

2.2. Producing MNTs with a Truncated Carrier Module

 doi:10.20944/preprints202407.1330.v1

To create MNT with a truncated carrier module, the previously described construct (DTox-HMP-NLS-EGF) was used. The MNT consists of the sequence of human epidermal growth factor (EGF) as a ligand module. The diphtheria toxin translocation domain (DTox) sequence was employed as an endosomolytic module. The sequence of the hemoglobin-like HMP protein was taken as a carrier module. The optimized nuclear localization signal (NLS) of the large T-antigen of the SV40 virus was used as a module for delivery into the cell nucleus. The gene encoding this MNT was deleted in the sections corresponding to two parts (C- or N-terminal) of the HMP sequence. Mutagenesis was performed using oligonucleotide primers by PCR amplification of the original gene without the corresponding fragments. The primers were synthesized by Evrogen, Moscow, Russia, and mutagenesis was performed using the QuickChange™ kit (Agilent Technologies, Santa Clara, CA, USA). Competent cells (XL1-Gold) were transformed with the obtained plasmids and grown in a SOC (Super Optimal Broth and Catabolic Repressor) medium overnight at 37 °C in the presence of ampicillin. Colonies with mutations were selected by PCR screening according to a standard protocol [26]. Furthermore, restriction analysis was used to determine whether a deletion happened in the areas of interest [27]. The obtained plasmids were sequenced using the Sanger technique [28].

2.3. MNT Expression and Purification

The production of DTox-HMP$_C$-NLS-EGF (MNT$_C$) with the C-terminal fragment of HMP, DTox-HMP$_N$-NLS-EGF (MNT$_N$) with the N-terminal fragment of HMP, and the original MNT (DTox-HMP-NLS-EGF, hereinafter referred to as the MNT$_F$) was carried out in the strain E. coli BCL-12. The cells were grown on LB Broth Miller medium (Amresco, Solon, OH, USA). The induction of MNT expression was performed with 200 μM of isopropyl-β-D-galactopyranoside (SybEnzyme, Russia) for 2.5 hours at 18 °C. All MNTs were isolated from the soluble fraction and purified by affinity chromatography on a HisTrap™ High Performance carrier (Cytiva, USA). Purified MNTs were refolded in 150 mM NaCl, 25 mM Na_2HPO_4, 0.5 mM phenylmethylsulfonyl fluoride, 1 mM EDTA, 2 mM oxidized glutathione, and 0.67 mM reduced glutathione. After refolding, the MNTs were re-purified by affinity chromatography and dialyzed against PBS (10 mM Na_2HPO_4, 150 mM NaCl, pH 8). The purity of MNTs produced using the given approach was approximately 85%, according to denaturing electrophoresis data. The concentration of MNT was assessed using the Bradford method [29].

2.4. Binding Assay

The effectiveness of the interaction of the ligand module with the epidermal growth factor receptor (EGFR) was evaluated on the cell line of human epidermal carcinoma A431, characterized by overexpression of EGFR. To do this, we determined the dissociation constant of the ligand-receptor complex in competition with a fluorescently labeled MNT$_1$ [18]. MNT$_1$ was labeled with Alexa-647 as described earlier [30]. Briefly, A freshly prepared solution of Alexa Fluor 647 succinimidyl ester (Molecular Probes, Eugene, OR, USA) (2 mg/mL) was added to the MNT$_1$ solution in carbonate buffer, pH 8.6 in molar excess of 5:1. Labeled MNT$_1$ was purified by ultrafiltration. Binding analysis was performed on A431 cells, which were dispersed onto 48-well plates and fixed with a 0.5% paraformaldehyde solution for 5 minutes on ice. Incubation with MNTs was performed in DMEM (Dulbecco's Modified Eagle Medium) medium containing 1% bovine serum albumin (BSA), 100 μg/ml gentamicin, 0.4 g/l $NaHCO_3$, 15 mM HEPES, pH 7.3, overnight at +4 °C. For the study of competitive binding, 25 nM of labeled MNT1 and different concentrations of MNTC or MNTN were used. After incubation, the cells were washed five times with Hanks solution, and 100 μl of 0.25% trypsin-EDTA solution per well was added for 2 hours. The well contents were removed to a black-well plate, and the wells were rinsed with 150 μl of a 1% Triton X-100 solution. Sample fluorescence was measured in the 630–680 nm range using a ClarioSTAR Plus plate reader (BMG LABTECH, Germany) with an excitation wavelength of 625–630 nm.

2.4. Liposome Leakage Assay

 doi:10.20944/preprints202407.1330.v1

The ability of MNT1 to provide liposome leakage was demonstrated on small unilamellar phosphatidylcholine (Sigma-Aldrich, Burlington, MA, USA) liposomes prepared by reverse-phase evaporation [31] loaded with the fluorescent dye calcein (Fluka, Seelze, Germany) to a concentration of 100 mM, which led to fluorescence self-quenching. Liposome leakage analysis was performed as described previously [18].

2.5. Thermophoresis

Binding between Keap1 and MNTs was assessed using a Monolith NT.115 instrument (NanoTemper Technologies, Munchen, Germany) in phosphate buffer containing sodium phosphate (25 mM) and sodium chloride (150 mM), pH 8.0, using Cy3-labeled Keap1, as described in our previous article [18].

The interaction of the MNTs with the α/β importin complex was evaluated in buffer containing 20 mM HEPES, 110 mM KCl, 5 mM NaHCO3, 5 mM $MgCl_2$, 0.1 mM $CaCl_2$, 1 mM EGTA, and 1 mM DTT, pH 7.4, using Cy3-labeled β-importin as described earlier [32].

2.7. Photocytotoxicity

Chlorin e_6 (Frontier Scientific, Philadelphia, PA, USA) was coupled to MNT using 1-ethyl-3-(3-dimethylaminopropyl)-carbodiimide and N-hydroxysuccinimide (Sigma-Aldrich) as described previously [18]. Briefly, a 3 mM aqueous solution of sodium chlorin e_6 was diluted in buffer containing 10 mM MES (Sigma-Aldrich), pH 6.5, and 1 mM sodium dodecyl sulfate (SDS-Na) to a final concentration of 150 μM. The resulting solution was mixed with freshly prepared 0.1 M aqueous solutions of 1-ethyl-3-(3-dimethylaminopropyl)-carbodiimide (Sigma-Aldrich) and N-hydroxysuccinimide (Sigma-Aldrich) up to the molar ratio clorin: carbodiimide:N-hydroxysuccinimide = 1:4.5:15. The solution of the activated chlorin e_6 was added to 10 μM of MNTs in buffer containing 30 mM sodium phosphate, 20 mM sodium borate, 150 mM sodium chloride, pH 8.0, and SDS-Na in the molar ratio MNT:SDS-Na = 1:5. The reaction was stopped the next day with hydroxylamine (Reakhim, Moscow, Russia) at a final concentration of 10 mM. The conjugates were purified using affinity chromatography on Ni-NTA Sepharose.

A431 cells were seeded in 96-well plates (1000 cells per well) for the cytotoxicity experiment. The next day, the media was changed to DMEM with 10 mg/mL BSA, and the cells were treated with various doses of MNT-chlorin conjugates or free chlorin e_6. After 20 hours of incubation, the cells were washed twice with Hank's solution and irradiated for 10 minutes (0.0276 W/cm2) with a slide projector in Hank's solution. Hank's solution was then replaced with fresh medium containing 10% fetal bovine serum and incubated for 4-5 days. Cell viability was assessed using 3-(4,5-dimethylthiazol-2-yl)-2,5- diphenyltetrazolium bromide (MTT). The experiments were repeated six times, and each of them was performed in six replicates. The concentration causing 50% cell death (EC_{50}) was estimated using data interpolation along a four-parameter logistic curve in the GraphPad Prism 9 software package (GraphPad Software Inc., La Jolla, CA, USA). The significance of the differences was assessed using ANOVA with the Prism software.

3. Results

For the study, plasmids encoding MNT with C-terminal and N-terminal parts of the carrier module were obtained. Both truncated MNTs were successfully produced and purified, as described in the "Materials and Methods" section.

A study of the binding of fluorescently labeled MNT1 showed that it binds to EGFR on the surface of A431 cells with a dissociation constant, K_d 46±15 nM (mean±SEM) (Figure 1a). This value is consistent with the data obtained by radioligand analysis (62±10 nM) [18]. Competitive analysis yielded K_d values of 10 ± 2 nM for MNT_C and 20 ± 4 nM for MNT_N (Figure 1b and 1c). This demonstrates that the ligand module in both MNTs retains functionality and can target MNT cells with overexpressed EGFR.

 doi:10.20944/preprints202407.1330.v1

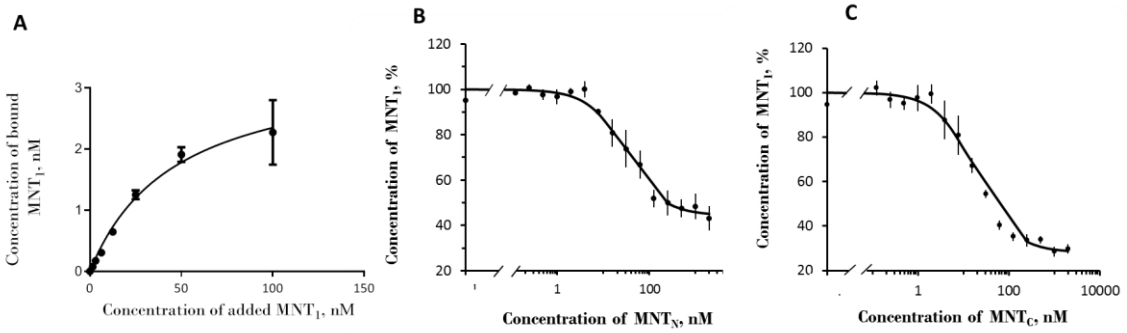

Figure 1. Binding of MNTs to EGFR of A431 cells. (**A**) binding of Alexa647-MNT1 to A431 cells; (**B**) and (**C**) represent concurrent binding of Alexa647-MNT1 to MNTN and MNTC, respectively. The data of typical experiments performed in three repetitions is presented. The data are presented as average values ± SEM.

Figure 2 shows the leakage of the fluorescent dye calcein from phosphatidylcholine liposomes at different pH levels. The experiments have shown that the new MNTs have membranolytic activity in the pH 5–6 region corresponding to the pH of the endosomes, which makes it possible to release MNTs from early endosomes after internalization.

Presumably, HMP participates in the membranolytic activity of MNT, and its truncation could lead to a decrease in this activity in the area of slightly acidic pH. As shown in Figure 2, MNT containing the N-terminal HMP domain exhibits somewhat less activity in this range. At pH 6, MNTN releases approximately 45% of calcein, while MNT with full-size HMP releases nearly 60%. Despite this, it appears that the loss of one of the HMP domains has no significant impact on MNT-membrane interaction.

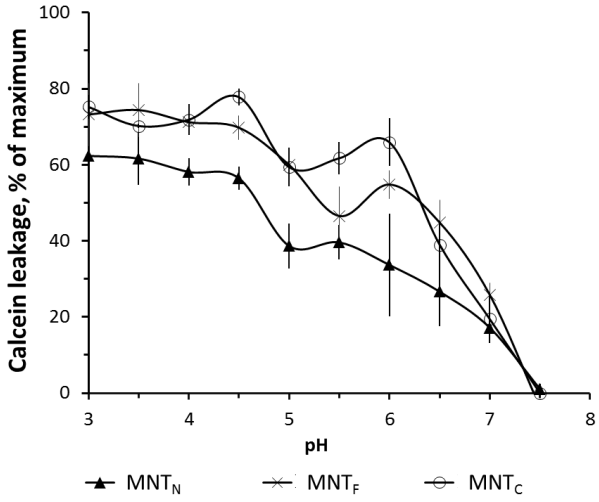

Figure 2. MNT-induced dye leakage from phosphatidylcholine liposomes loaded with the fluorescent dye calcein to the fluorescence self-quenching concentration. The data are mean values ± SEM.

The thermophoresis assay makes it possible to observe a change in the diffusion rate of molecules during the formation of complexes due to the registration of fluorescence by one of the interacting substances.

Thermophoretic curves for MNTN and MNTC are shown in Figure 3a,b, respectively. The results of the experiments demonstrated that MNTN with N-terminal domain of HMP interacts with Keap1 with K_d of 428 ± 193 nM. At the same time, MNTC, has a much higher dissociation constant of the complex with Keap1 (K_d = 1800 ± 500 nM). The difference between the measured values of the

 doi:10.20944/preprints202407.1330.v1

dissociation constants is significant ($p < 0.05$, $n = 12$). In addition, the values of dissociation constants for MNT_C and MNT_F with full-size HMP (205 ± 22 nM) differ significantly (Figure 3). At the same time, the difference in dissociation constants for MNT_F and MNT_C is nonsignificant. Thus, it can be concluded that HMP interacts with Keap1 due to the N-terminal (globin) part.

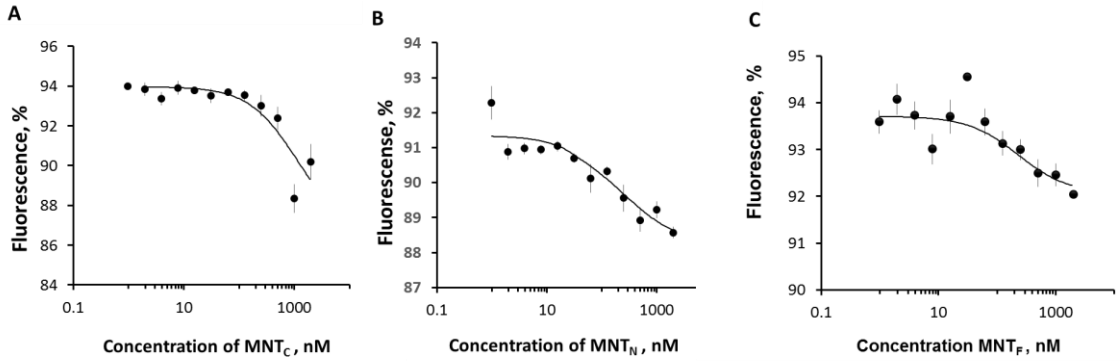

Figure 3. The interaction of MNTs with Keap1-Cy3 assessed by thermophoresis. Dependences of relative fluorescence intensities (fluorescence intensity before the start of thermophoresis is taken as 100%) at 20 s after the start of thermophoresis on the concentration of the MNT_C (**A**), MNT_N (**B**) and MNT_C (**C**) at a constant concentration of the Keap1-Cy3. Standard errors (SE) of relative fluorescence intensities are shown (n = 12).

The thermophoretic curves of the interaction of MNTs with α/β-importins are shown in Figure 4. The dissociation constants of the new constructs with the complex of imports were 160 ± 31 nM and 179 ± 22 nM for MNT_N and MNT_C, respectively. This demonstrates that modules for delivery to the nucleus of these MNTs are functional, allowing these MNTs to be delivered into the cell nucleus.

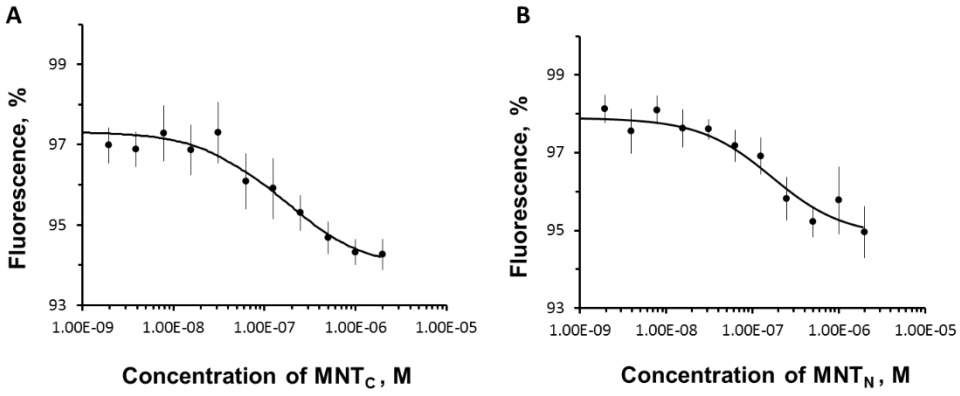

Figure 4. The interaction of MNTs with α/β importin complex labeled with Cy3 assessed by thermophoresis. Dependences of relative fluorescence intensities (fluorescence intensity before the start of thermophoresis is taken as 100%) at 20 s after the start of thermophoresis on the concentration of MNT_N (**A**) and MNT_C (**B**) at a constant concentration of the importin complex. Standard errors (SE) of relative fluorescence intensities are shown (n = 7-9).

The effectiveness of the photosensitizer was assessed by the concentration of MNT, which causes the death of 50% of cells. Figure 5 shows the results of a comparison of the effects on cells of two new MNTs and the original MNT_F with the attached chlorin *e*6. For MNT_C, the EC_{50} was 6 ± 3.4 nM, and for MNT_N, it was 1.3 ± 0.5 nM. The EC_{50} of free chlorin *e*6 was about 550 ± 110 nM, which shows that truncated structures significantly enhance the photodynamic effect of chlorin e6 on A431 cells. For the original MNT_F with a full-size carrier module, the EC_{50} was 13.7 ± 3.6 nM; that is, the new constructs destroy cells more efficiently. At the same time, the significance of differences from the effect of the original MNT_F was revealed only for MNT_N with the N-terminal part of HMP ($p = 0.015$).

 doi:10.20944/preprints202407.1330.v1

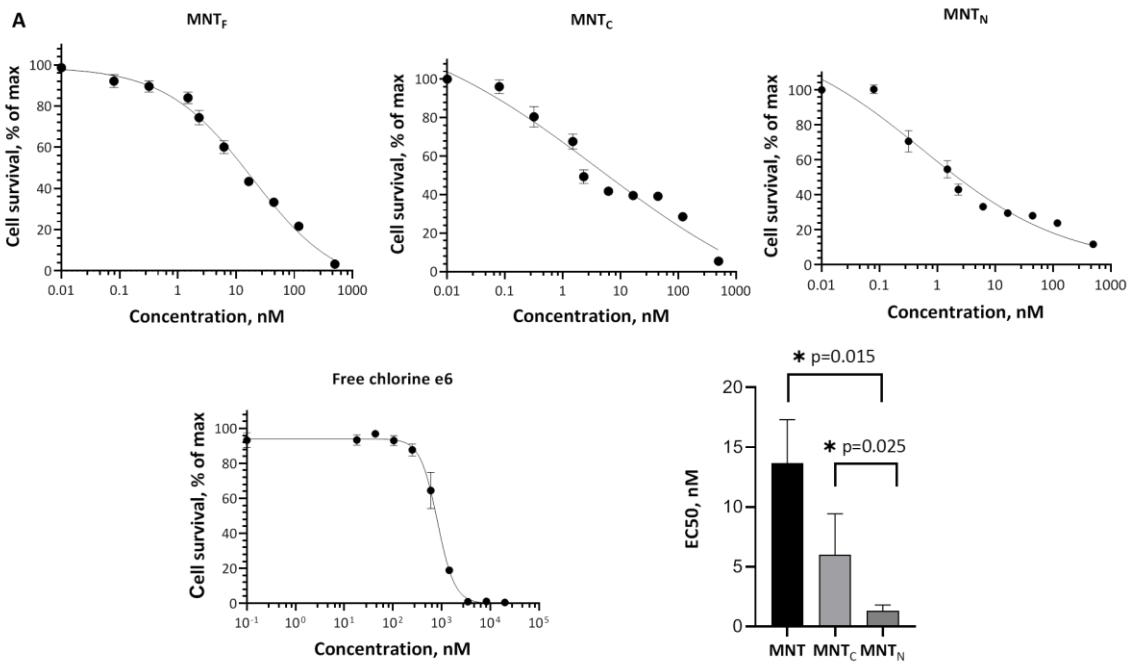

Figure 5. Photocytotoxicity of MNTF-chlorin e_6 (A), MNTc-chlorin e_6 (B), MNTN-chlorin e_6 (C) and free chlorin e_6 (D) on A431 cells. Experimental data of six experiments (circles) fitted using the four-parameter logistic sigmoid curves (lines) are given. EC_{50} values derived from sigmoid model approximation for each conjugate (E). Error bars represent standard errors (n = 6).

4. Discussion

When creating or modifying complex transport structures for intracellular delivery to target cells, it is necessary to ensure that all components of these structures retain their functionality. Due to the ligand module, which is able to bind to EGFR, MNT is able to recognize cancer cells and penetrate them via receptor-mediated endocytosis. As previous work has shown, the K_d for MNT_F with a full-size carrier module is 29 nM [17]. In experiments on A431 cells carrying an increased number of these receptors, it was shown that truncated constructs retain the ability to bind to EGFR receptors on the cell surface, forming MNT-receptor complexes with dissociation constants of about 10 and 20 nM, respectively. This binding of new MNT with EGFR suggests that they are able to successfully penetrate target cells by receptor-mediated endocytosis.

The endosomal activity of the new transporters was assessed by their ability to disrupt the integrity of lipid membranes in a model system of liposomes loaded with calcein. The membranolytic properties of MNT reflect the release of calcein from liposomes during incubation with MNT at different pHs. The main role in the ability of MNT to destroy membranes is played by the translocation T domain of the diphtheria toxin, which, with a decrease in pH, is able to change its conformation and integrate into the lipid bilayer [33–35]. Previous research has also demonstrated HMP's potential to attach to lipid membranes and its membranolytic activity in the pH range of 3–4. The occurrence of two peaks on the pH curve of the dependency of MNT's endosomolytic activity may be attributed to the joint action of two modules: one emerges as a result of HMP action, while the other is DTox [17]. According to atomic force microscopy studies of lipid membranes incubated with MNT, the combined action of HMP and DTox most likely results in the formation of ring-shaped structures on the surface of lipid membranes that contain MNT embedded in the membrane and ensure MNT release from endosomes [17]. MNT_N containing only the N-terminal part of HMP exhibits decreased membranolytic action. In this regard, it can be assumed that the C-terminal fragment of HMP also plays an important role in this module's endosomolytic activity, providing endosomolytic activity in the pH 3–4 region while also causing MNT to be incorporated into the membrane and pores to form in the pH 5–6 region. Membranolytic activity of the globin N-terminal

 doi:10.20944/preprints202407.1330.v1

domain of HMP is more expected [36]. Nevertheless, the effect of MNT_N on lipid membranes is sufficient to lead to their destruction at a slightly acidic pH. Thus, when the contents of the endosomes are acidified, both MNTs are able to disturb the lipid bilayer.

The nucleus is an important target for many drugs as it contains DNA, damage to which, as a rule, leads to cell death [37–40]. The ability to bind to importins that allow proteins with NLS to penetrate into the nucleus through the nuclear pore, as shown by thermophoresis, indicates the possibility of successful penetration of MNT with N- and C-terminal parts of the carrier module into the nucleus.

In this article, we also investigated how the previously discovered interaction of the MNT carrier module with Keap1 can affect the effectiveness of the photodynamic action of a photosensitizer delivered to the cell nucleus. Kear1 is an Nrf2 inhibitor that controls the expression of most proteins involved in the metabolism of reactive oxygen species [41–43].

The displacement of Keap1 from the complex with Nrf2 can be used to activate the Nrf2 system of protection against oxidative stress [36], for example, with the help of antibodies to Keap1 [37]. For MNT targeted at Keap1 using the AntiKeap1 monobody antibody-like molecule, it has been shown that the interaction occurs both through the AntiKeap1 monobody and through HMP [7]. Now, by thermophoresis, it has been shown that MNT with N-NMR interacts with Keap1 in contrast to MNT with C-HMP, which suggests that the binding site of NMR to Keap1 is located in the N-terminal globin domain.

The displacement of Keap1 from the complex with Nrf2 can be used to activate the Nrf2 system of protection against oxidative stress [36], for example, with the help of peptides or antibodies against Keap1 [37]. For MNT targeted at Keap1 using the anti-Keap1monobody antibody-like molecule, it has been shown that the interaction occurs both through Anti-Keap1 monobody and through HMP [7]. Now, by thermophoresis, it has been shown that MNT with N-NMR interacts with Kear1 in contrast to MNT with C-end of HMP, which suggests that the binding site of HMP to Keap1 is located in its N-terminal globin domain.

The displacement of Keap1 from the complex with Nrf2 can be used to activate the Nrf2 system of protection against oxidative stress [44], for example, with the help of peptides or antibodies against Keap1 [45–47]. For MNT targeted at Keap1 using the anti-Keap1 monobody antibody-like molecule, it has been shown that the interaction occurs both through the anti-Keap1 monobody and through HMP [18]. Now, by thermophoresis, it has been shown that MNT with N-NMR interacts with Kear1 in contrast to MNT with the C-end of HMP, which suggests that the binding site of HMP to Keap1 is located in its N-terminal globin domain.

Our study shows that truncation of the HMP carrier module does not affect the functional activity of the MNT. Moreover, transporters with a truncated carrier module demonstrated a more pronounced photodynamic effect on A431 cells compared to MNT with full-size HMP. This may indicate that they carry out a more efficient delivery of the photosensitizer to vulnerable cell compartments. It is possible that the size of MNT plays a significant role in penetration into cells and cellular compartments; therefore, both MNT and truncated HMP turned out to be more cytotoxic as carriers of photosensitizers. The hemoglobin-like E. coli protein (HMP), used as a carrier module in MNT, belongs to the flavohemoglobin group. Although it is believed that the main role of HMP in bacterial cells is to neutralize NO radicals under aerobic and anaerobic conditions [48], the processes occurring in this case are still not fully understood. HMP consists of two domains: N-terminal globin and C-terminal reductase, both of which perform their function in the process of neutralizing NO [49]. HMP has been shown to exhibit enzymatic activity in human cells; for example, it has been used to study the functions of NO signaling in mammalian cells. The expression of flavohemoglobins led to increased resistance to NO-induced cell death and weakened various NO-signaling pathways [50]. According to some reports, HMP proteins are able to protect bacteria not only from nitrosative stress but also from oxidative stress caused by ROS. A number of structural features of HMP indicate the similarity of this protein to peroxidases [50, 51]. It has also been shown that mutant bacteria lacking the gene encoding HMP are less resistant to oxidative stress [52], although its overexpression leads to the accumulation of peroxide and superoxide [53]. Purified MNT contains only a small

 doi:10.20944/preprints202407.1330.v1

fraction of heme, making it unlikely that HMP has enzymatic action in cells. Nonetheless, it is possible that these features of full-sized HMP can be observed in eukaryotic cells, potentially weakening the oxidative processes induced by photodynamic treatment. As both HMP domains operate together to achieve reductase activity, MNTF can be less effective than truncated MNTs.

Interaction with Keap1 at the same time, as it turned out, does not interfere with the delivery process but, on the contrary, gives MNT_N an advantage. It is known that Keap1 is localized, in particular, on the outer membrane of mitochondria [24, 25], in connection with which the alleged interaction of MNT with Kear1 may lead to the accumulation of a photosensitizer on the outer membrane of mitochondria. Damage to mitochondria is one of the important pathways leading to cell death under the action of photosensitizers. Thus, mitochondria-associated photosensitizers can cause photodamage of the membrane-bound protein Bcl-227, which can lead to the release of caspase activators such as cytochrome c and Smac/DIABLO, or other pro-apoptotic molecules, including apoptosis-inducing factor (AIF) [54].

Photosensitizers can cause cell death through three mechanisms: apoptosis, necrosis, and autophagy. Some photosensitizers target mitochondria specifically [15]. MNT targeting Keap1 with an anti-Keap1 monobody has been shown to boost photosensitizer efficiency by localizing on the mitochondrial membrane [18]. Thus, an increase in the cytotoxic effect of the N-terminal HMP transporter capable of binding to Keap1 may indicate that this MNT is being targeted in addition to the nucleus and mitochondria.

5. Conclusions

New MNTs obtained as a result of the truncation of the carrier module are able to recognize target cells, penetrate them, and have a cytotoxic effect when photosensitizers are attached to them. This work shows that the HMP carrier module in the structure can be significantly reduced, and the effectiveness of MNT as carriers of therapeutic drugs into cells does not decrease. In this case, it is preferable to leave the N-terminal part of the HMP capable of binding to Keap1 in the MNT.

Author Contributions: Conceptualization, A.A.R..; methodology, A.A.R., A.V.U., T.A.S., and Y.V.K.; investigation, R.T.A., M.A.G., A.A.R., T.A.S., A.V.U., and Y.V.K.; writing—original draft preparation, R.T.A.; writing—review and editing, A.A.R. and T.A.S..; visualization, R.T.A., A.A.R..; supervision, G.P.G.; funding acquisition, G.P.G.

Funding: The research was supported by the grant 22-14-00094 of the Russian Science Foundation.

Acknowledgments: These experiments were carried out with the use of equipment from the Center for Precision Genome Editing and Genetic Technologies for Biomedicine, IGB RAS. We are also grateful to the Lomonosov Moscow State University Program of Development for the use of its equipment.

Conflicts of Interest: The authors declare no conflicts of interest.

References

1. Lee, Y. T.; Tan, Y. J.; Oon, C. E. Molecular targeted therapy: Treating cancer with specificity. Eur. J. Pharmacol. 2018, 834, 188-196.
2. Manzari, M. T.; Shamay, Y.; Kiguchi, H.; Rosen, N.; Scaltriti, M.; Heller, D. A. Targeted drug delivery strategies for precision medicines. Nat. Rev. Mater. 2021, 6 (4), 351-370.
3. Craik, D. J.; Fairlie, D. P.; Liras, S.; Price, D. The future of peptide-based drugs. Chem. Biol. Drug Des 2013, 81 (1), 136-147.
4. Muttenthaler, M.; King, G. F.; Adams, D. J.; Alewood, P. F. Trends in peptide drug discovery. Nat. Rev. Drug Discov. 2021, 20 (4), 309-325.
5. Vargason, A. M.; Anselmo, A. C.; Mitragotri, S. The evolution of commercial drug delivery technologies. Nat. Biomed. Eng 2021, 5 (9), 951-967.
6. Wang, L.; Wang, N.; Zhang, W.; Cheng, X.; Yan, Z.; Shao, G.; Wang, X.; Wang, R.; Fu, C. Therapeutic peptides: current applications and future directions. Signal. Transduct. Target Ther. 2022, 7 (1), 48.
7. Sobolev, A. S. The Delivery of Biologically Active Agents into the Nuclei of Target Cells for the Purposes of Translational Medicine. Acta Naturae. 2020, 12 (4), 47-56.

8. Slastnikova, T. A.; Rosenkranz, A. A.; Gulak, P. V.; Schiffelers, R. M.; Lupanova, T. N.; Khramtsov, Y. V.; Zalutsky, M. R.; Sobolev, A. S. Modular nanotransporters: a multipurpose in vivo working platform for targeted drug delivery. Int. J. Nanomedicine. 2012, 7, 467-482.
9. Slastnikova, T. A.; Rosenkranz, A. A.; Lupanova, T. N.; Gulak, P. V.; Gnuchev, N. V.; Sobolev, A. S. Study of efficiency of the modular nanotransporter for targeted delivery of photosensitizers to melanoma cell nuclei in vivo. Dokl. Biochem. Biophys. 2012, 446, 235-237.
10. Rosenkranz, A. A.; Slastnikova, T. A.; Karmakova, T. A.; Vorontsova, M. S.; Morozova, N. B.; Petriev, V. M.; Abrosimov, A. S.; Khramtsov, Y. V.; Lupanova, T. N.; Ulasov, A. V.; Yakubovskaya, R. I.; Georgiev, G. P.; Sobolev, A. S. Antitumor Activity of Auger Electron Emitter (111)In Delivered by Modular Nanotransporter for Treatment of Bladder Cancer With EGFR Overexpression. Front Pharmacol. 2018, 9, 1331.
11. Slastnikova, T. A.; Koumarianou, E.; Rosenkranz, A. A.; Vaidyanathan, G.; Lupanova, T. N.; Sobolev, A. S.; Zalutsky, M. R. Modular nanotransporters: a versatile approach for enhancing nuclear delivery and cytotoxicity of Auger electron-emitting 125I. EJNMMI. Res. 2012, 2 (1), 59.
12. Correia, J. H.; Rodrigues, J. A.; Pimenta, S.; Dong, T.; Yang, Z. Photodynamic Therapy Review: Principles, Photosensitizers, Applications, and Future Directions. Pharmaceutics. 2021, 13 (9).
13. Li, X.; Lovell, J. F.; Yoon, J.; Chen, X. Clinical development and potential of photothermal and photodynamic therapies for cancer. Nat. Rev. Clin. Oncol. 2020, 17 (11), 657-674.
14. Kim, T. E.; Chang, J. E. Recent Studies in Photodynamic Therapy for Cancer Treatment: From Basic Research to Clinical Trials. Pharmaceutics. 2023, 15 (9).
15. Agostinis, P.; Berg, K.; Cengel, K. A.; Foster, T. H.; Girotti, A. W.; Gollnick, S. O.; Hahn, S. M.; Hamblin, M. R.; Juzeniene, A.; Kessel, D.; Korbelik, M.; Moan, J.; Mroz, P.; Nowis, D.; Piette, J.; Wilson, B. C.; Golab, J. Photodynamic therapy of cancer: an update. CA Cancer J. Clin. 2011, 61 (4), 250-281.
16. Huis In 't Veld RV; Heuts, J.; Ma, S.; Cruz, L. J.; Ossendorp, F. A.; Jager, M. J. Current Challenges and Opportunities of Photodynamic Therapy against Cancer. Pharmaceutics. 2023, 15 (2).
17. Gilyazova, D. G.; Rosenkranz, A. A.; Gulak, P. V.; Lunin, V. G.; Sergienko, O. V.; Khramtsov, Y. V.; Timofeyev, K. N.; Grin, M. A.; Mironov, A. F.; Rubin, A. B.; Georgiev, G. P.; Sobolev, A. S. Targeting cancer cells by novel engineered modular transporters. Cancer Res. 2006, 66 (21), 10534-10540.
18. Khramtsov, Y. V.; Ulasov, A. V.; Slastnikova, T. A.; Rosenkranz, A. A.; Lupanova, T. N.; Georgiev, G. P.; Sobolev, A. S. Modular Nanotransporters Delivering Biologically Active Molecules to the Surface of Mitochondria. Pharmaceutics. 2023, 15 (12).
19. Ilari, A.; Bonamore, A.; Farina, A.; Johnson, K. A.; Boffi, A. The X-ray structure of ferric Escherichia coli flavohemoglobin reveals an unexpected geometry of the distal heme pocket. J. Biol. Chem. 2002, 277 (26), 23725-23732.
20. Dreher, M. R.; Liu, W.; Michelich, C. R.; Dewhirst, M. W.; Yuan, F.; Chilkoti, A. Tumor vascular permeability, accumulation, and penetration of macromolecular drug carriers. J. Natl. Cancer Inst. 2006, 98 (5), 335-344.
21. Suzuki, T.; Takahashi, J.; Yamamoto, M. Molecular Basis of the KEAP1-NRF2 Signaling Pathway. Mol. Cells 2023, 46 (3), 133-141.
22. Yamamoto, M.; Kensler, T. W.; Motohashi, H. The KEAP1-NRF2 System: a Thiol-Based Sensor-Effector Apparatus for Maintaining Redox Homeostasis. Physiol Rev. 2018, 98 (3), 1169-1203.
23. Hayes, J. D.; Dinkova-Kostova, A. T. The Nrf2 regulatory network provides an interface between redox and intermediary metabolism. Trends Biochem. Sci. 2014, 39 (4), 199-218.
24. Kopacz, A.; Kloska, D.; Forman, H. J.; Jozkowicz, A.; Grochot-Przeczek, A. Beyond repression of Nrf2: An update on Keap1. Free Radic. Biol. Med. 2020, 157, 63-74.
25. Lo, S. C.; Hannink, M. PGAM5 tethers a ternary complex containing Keap1 and Nrf2 to mitochondria. Exp. Cell Res. 2008, 314 (8), 1789-1803.
26. Trower, M. K. A rapid PCR-based colony screening protocol for cloned inserts. Methods Mol. Biol. 1996, 58, 329-333.
27. Ota, M.; Asamura, H.; Oki, T.; Sada, M. Restriction enzyme analysis of PCR products. Methods Mol. Biol. 2009, 578, 405-414.
28. Sanger, F.; Nicklen, S.; Coulson, A. R. DNA sequencing with chain-terminating inhibitors. Proc. Natl. Acad. Sci. U. S. A 1977, 74 (12), 5463-5467.
29. Bradford, M. M. A rapid and sensitive method for the quantitation of microgram quantities of protein utilizing the principle of protein-dye binding. Anal. Biochem. 1976, 72, 248-254.
30. Slastnikova, T. A.; Rosenkranz, A. A.; Ulasov, A. V.; Khramtsov, Y. V.; Lupanova, T. N.; Georgiev, G. P.; Sobolev, A. S. Mouse Syngeneic Melanoma Model with Human Epidermal Growth Factor Receptor Expression. Pharmaceutics. 2022, 14 (11).
31. Szoka, F., Jr.; Papahadjopoulos, D. Procedure for preparation of liposomes with large internal aqueous space and high capture by reverse-phase evaporation. Proc. Natl. Acad. Sci. U. S. A 1978, 75 (9), 4194-4198.

 doi:10.20944/preprints202407.1330.v1

32. Karyagina, T. S.; Ulasov, A. V.; Slastnikova, T. A.; Rosenkranz, A. A.; Lupanova, T. N.; Khramtsov, Y. V.; Georgiev, G. P.; Sobolev, A. S. Targeted Delivery of (111)In Into the Nuclei of EGFR Overexpressing Cells via Modular Nanotransporters With Anti-EGFR Affibody. Front Pharmacol. 2020, 11, 176.
33. Ladokhin, A. S. pH-triggered conformational switching along the membrane insertion pathway of the diphtheria toxin T-domain. Toxins. (Basel) 2013, 5 (8), 1362-1380.
34. Leka, O.; Vallese, F.; Pirazzini, M.; Berto, P.; Montecucco, C.; Zanotti, G. Diphtheria toxin conformational switching at acidic pH. FEBS J 2014, 281 (9), 2115-2122.
35. Rodnin, M. V.; Kyrychenko, A.; Kienker, P.; Sharma, O.; Posokhov, Y. O.; Collier, R. J.; Finkelstein, A.; Ladokhin, A. S. Conformational switching of the diphtheria toxin T domain. J Mol. Biol. 2010, 402 (1), 1-7.
36. Di, G. A.; Bonamore, A. Globin interactions with lipids and membranes. Methods Enzymol. 2008, 436, 239-253.
37. Sui, M.; Liu, W.; Shen, Y. Nuclear drug delivery for cancer chemotherapy. J. Control Release 2011, 155 (2), 227-236.
38. Pan, L.; Liu, J.; Shi, J. Cancer cell nucleus-targeting nanocomposites for advanced tumor therapeutics. Chem. Soc. Rev. 2018, 47 (18), 6930-6946.
39. Tiwari, R.; Jain, P.; Asati, S.; Haider, T.; Soni, V.; Pandey, V. State-of-art based approaches for anticancer drug-targeting to nucleus. Journal of Drug Delivery Science and Technology 2018, 48, 383-392.
40. Goyal, P.; Malviya, R. Advances in nuclei targeted delivery of nanoparticles for the management of cancer. Biochim. Biophys. Acta Rev. Cancer 2023, 1878 (3), 188881.
41. Bellezza, I.; Giambanco, I.; Minelli, A.; Donato, R. Nrf2-Keap1 signaling in oxidative and reductive stress. Biochim. Biophys. Acta Mol. Cell Res. 2018, 1865 (5), 721-733.
42. Nguyen, T.; Nioi, P.; Pickett, C. B. The Nrf2-antioxidant response element signaling pathway and its activation by oxidative stress. J. Biol. Chem. 2009, 284 (20), 13291-13295.
43. Baird, L.; Dinkova-Kostova, A. T. The cytoprotective role of the Keap1-Nrf2 pathway. Arch. Toxicol. 2011, 85 (4), 241-272.
44. Suzuki, T.; Motohashi, H.; Yamamoto, M. Toward clinical application of the Keap1-Nrf2 pathway. Trends Pharmacol Sci 2013, 34 (6), 340-346.
45. Guntas, G.; Lewis, S. M.; Mulvaney, K. M.; Cloer, E. W.; Tripathy, A.; Lane, T. R.; Major, M. B.; Kuhlman, B. Engineering a genetically encoded competitive inhibitor of the KEAP1-NRF2 interaction via structure-based design and phage display. Protein Eng Des Sel 2016, 29 (1), 1-9.
46. Mou, Y.; Wen, S.; Li, Y. X.; Gao, X. X.; Zhang, X.; Jiang, Z. Y. Recent progress in Keap1-Nrf2 protein-protein interaction inhibitors. Eur. J Med Chem. 2020, 202, 112532.
47. Ulasov, A. V.; Rosenkranz, A. A.; Georgiev, G. P.; Sobolev, A. S. Nrf2/Keap1/ARE signaling: Towards specific regulation. Life Sci 2022, 291, 120111.
48. Nath, R.; Sengupta, S.; Bhattacharjee, A. Enzymatic and Non-Enzymatic Response during Nitrosative Stress in. Post-Щру Mikrobiologii-Advancements of Microbiology 2022, 61 (2), 81-93.
49. Poole, R. K.; Hughes, M. N. New functions for the ancient globin family: bacterial responses to nitric oxide and nitrosative stress. Mol. Microbiol. 2000, 36 (4), 775-783.
50. Forrester, M. T.; Eyler, C. E.; Rich, J. N. Bacterial flavohemoglobin: a molecular tool to probe mammalian nitric oxide biology. Biotechniques 2011, 50 (1), 41-45.
51. Mukai, M.; Mills, C. E.; Poole, R. K.; Yeh, S. R. Flavohemoglobin, a globin with a peroxidase-like catalytic site. J Biol. Chem. 2001, 276 (10), 7272-7277.
52. Membrillo-Hernandez, J.; Coopamah, M. D.; Anjum, M. F.; Stevanin, T. M.; Kelly, A.; Hughes, M. N.; Poole, R. K. The flavohemoglobin of Escherichia coli confers resistance to a nitrosating agent, a "Nitric oxide Releaser," and paraquat and is essential for transcriptional responses to oxidative stress. J Biol. Chem. 1999, 274 (2), 748-754.
53. Frey, A. D.; Farres, J.; Bollinger, C. J.; Kallio, P. T. Bacterial hemoglobins and flavohemoglobins for alleviation of nitrosative stress in Escherichia coli. Appl. Environ. Microbiol. 2002, 68 (10), 4835-4840.
54. Buytaert, E.; Dewaele, M.; Agostinis, P. Molecular effectors of multiple cell death pathways initiated by photodynamic therapy. *Biochim. Biophys. Acta* **2007,** *1776* (1), 86-107.